



Modeling spatiotemporal CO₂ (carbon dioxide) emission dynamics in China from DMSP-OLS nighttime stable light data using panel data analysis



Kaifang Shi ^{a,b}, Yun Chen ^b, Bailang Yu ^{a,*}, Tingbao Xu ^c, Zuoqi Chen ^a, Rui Liu ^{a,b}, Linyi Li ^d, Jianping Wu ^a

^a Key Laboratory of Geographic Information Science, Ministry of Education, East China Normal University, Shanghai 200241, China

^b CSIRO Land and Water, Canberra 2601, Australia

^c Fenner School of Environment and Society, The Australian National University, Linnaeus Way, Canberra 2601, Australia

^d School of Remote Sensing and Information Engineering, Wuhan University, Wuhan 430079, China

HIGHLIGHTS

- A true correlation between NSL data and statistical CO₂ emissions was proved.
- Spatiotemporal CO₂ emission dynamics at 1 km resolution in China were modeled.
- CO₂ emissions from national down to urban agglomeration scales were analyzed.

ARTICLE INFO

Article history:

Received 29 May 2015

Received in revised form 27 November 2015

Accepted 28 November 2015

Keywords:

CO₂ emissions

Spatiotemporal dynamics

DMSP-OLS

Panel data analysis

China

ABSTRACT

China's rapid industrialization and urbanization have resulted in a great deal of CO₂ (carbon dioxide) emissions, which is closely related to its sustainable development and the long term stability of global climate. This study proposes panel data analysis to model spatiotemporal CO₂ emission dynamics at a higher resolution in China by integrating the Defense Meteorological Satellite Program's Operational Linescan System (DMSP-OLS) nighttime stable light (NSL) data with statistic data of CO₂ emissions. Spatiotemporal CO₂ emission dynamics were assessed from national scale down to regional and urban agglomeration scales. The evaluation showed that there was a true positive correlation between NSL data and statistic CO₂ emissions in China at the provincial level from 1997 to 2012, which could be suitable for estimating CO₂ emissions at 1 km resolution. The spatiotemporal CO₂ emission dynamics between different regions varied greatly. The high-growth type and high-grade of CO₂ emissions were mainly distributed in the Eastern region, Shandong Peninsula and Middle south of Liaoning, with clearly lower concentrations in the Western region, Central region and Sichuan–Chongqing. The results of this study will enhance the understanding of spatiotemporal variations of CO₂ emissions in China. They will provide a scientific basis for policy-making on viable CO₂ emission mitigation policies.

© 2015 Elsevier Ltd. All rights reserved.

1. Introduction

Climate warming has become an enormous threat to the natural environment and human society in the world [1,2]. In addition to natural factors, global climate warming is closely related to CO₂ (carbon dioxide) emissions produced by human socio-economic activities [3,4]. Over the past century, continuously increasing population and economic development directly induced a high-rise of CO₂ emissions all over the world, especially in rapidly developing countries [5].

China has been undergoing an accelerated growth in industrialization and urbanization since the start of its economic reforms in 1978. This growth inevitably leads to a large volume of CO₂ emissions that threatens China's sustainable development and the long term stability of global climate [6–8], which has raised global concerns. According to 2010 Statistics of the United Nations, China has surpassed the United States to become the leading country of CO₂ emissions in the world [9]. Most importantly, due to industrial transition and the long-term durative influence of economic growth, China's CO₂ emissions will increase unceasingly [10]. Yet, China is encountering intense pressure to reduce its CO₂ emissions [11,12]. Hence, accurately measuring spatiotemporal CO₂ emission dynamics in China is a critical prerequisite for making evidence-based decisions on where and how to reduce CO₂ emissions.

* Corresponding author.

E-mail address: blyu@geo.ecnu.edu.cn (B. Yu).

Previous studies have modeled spatiotemporal CO₂ emission dynamics in China and elsewhere in several ways. For example, Clarke-Sather et al. [13] estimated inter-provincial inequality in CO₂ emissions in China for 1997–2007. Cheng et al. [10] analyzed spatiotemporal dynamics and dominating factors of China's CO₂ intensity from energy consumption for 1997–2010. Using logarithmic comparison and Kaya identical equation, Gingrich et al. [14] presented fossil-fuel related CO₂ emissions in Austria and Czechoslovakia for 1830–2000. However, most previous investigations in this field have used statistical data based on administrative units. In spite of their authoritativeness, the statistical data only provide numeric records of CO₂ emissions for an entire administrative unit without showing internal spatial patterns [15]. Due to the absence of spatial distributions, the spatiotemporal CO₂ emission dynamics within an administrative unit have not been clarified. Consequently, more efficient and economical methods should be used to couple with statistical data for mapping spatiotemporal CO₂ emission dynamics [16].

Satellite remote sensing imagery can provide spatial details for describing the spatiotemporal dynamics of fauna, flora and human societies [17–19]. Previous studies have demonstrated that the nighttime light data obtained by the Defense Meteorological Satellite Program's Operational Linescan System (DMSP-OLS) have a great potential to estimate socioeconomic indicators [15,16,20–24,6,25], and thus can be integrated with statistical data for capturing spatiotemporal CO₂ emission dynamics [2,26,27]. For example, using the DMSP-OLS data and statistical CO₂ emissions, Meng et al. [28] proposed a top-down method to map CO₂ emissions at urban scales. Lu et al. [2] utilized spatially distributed information from the DMSP-OLS data and a human activity index to test the hypothesis that countries with similar CO₂ emissions were spatially clustered. Su et al. [9] developed a normalized method for estimating China's 19-years CO₂ emissions using the DMSP-OLS data and explored major driving forces for proposing feasible mitigation policies. While the modeling of CO₂ emissions reported in these studies used a range of methods, most results were derived from simple regression methods, including linear regression model [16,25], power regression model [15] and log–log regression model [19,6]. Due to lack of data verification, the reported regression between statistical CO₂ emissions and nighttime light data could be spurious [29]. Moreover, simple regression methods merely quantify the relationship either in spatial dimension, or temporal dimension, which could result in bias in estimating CO₂ emissions from both spatial and temporal domains.

Panel data analysis is a method of endowing regression analysis in both spatial and temporal dimensions, which has many advantages over the simple regression analysis [30]. For example, panel unit root test can examine the stationary nature of the variables to avoid the spurious regression. A long-run equilibrium relationship between the variables can be determined by a panel cointegration test. Panel data models also make more sample variabilities and more degrees of freedom available, which can increase the estimation efficiency [3,31]. Thus, panel data analysis has enabled researchers to undertake longitudinal and horizontal analyses in a wide variety of fields, such as economics [32], geography [33], politics [34], and education [35].

This study aims to test the utility of modeling spatiotemporal CO₂ emission dynamics in China from DMSP-OLS data using panel data analysis for 1997–2012. The contributions of this study are summarized as follows:

- The panel data analysis proved that there was a true positive correlation between DMSP-OLS data and statistical CO₂ emissions in China at the provincial level for 1997–2012.
- CO₂ emission dynamics at 1 km resolution in China were modeled using DMSP-OLS data and statistical CO₂ emissions.

- CO₂ emission dynamics from national scale down to regional and urban agglomeration scales were identified and analyzed.

The remainder of this study is organized as follows. Section 2 describes the study areas and data sources. Section 3 introduces the methodology used. Section 4 analyzes the results of panel data analysis and spatiotemporal CO₂ emission dynamics in China. Section 5 presents an accuracy assessment and suggestions for China's CO₂ emission mitigation. The conclusions are given in Section 6.

2. Study areas and data sources

2.1. Study areas

Study areas were selected from three different administrative levels for multi-scales analysis. The first level is at national scale (Fig. 1). Since its reform and opening up, China has been experiencing a dramatic increase in gross domestic product (GDP), from 365 billion RMB in 1978 to 51,628 billion RMB in 2012. This enormous economic growth has led to a large amount of natural resource consumption, and a vast volume of CO₂ emissions. The second level is at regional scale. Due to China's uneven socioeconomic development, different economic regions with great disparities of CO₂ emissions have been formed. In this study, the entire mainland of China was divided into three regions (Eastern region, Central region and Western region) based on their socioeconomic development and geographical position (Figs. 1 and 2). The third level is at urban agglomeration scale (Fig. 1). Since China's population growth and economic development are concentrated in some urban agglomerations, these regions would contribute most to CO₂ emissions in China. In this study, six typical urban agglomerations, including Shanghai–Nanjing–Hangzhou, Pearl River Delta, Beijing–Tianjin–Tangshan, Middle south of Liaoning, Shandong Peninsula, and Sichuan–Chongqing, were selected as study areas. These urban agglomerations had the higher density of population and GDP than those of other areas in China. As shown in Fig. 2, the average percentages of population and GDP for 1997–2012 accounted 5.5% and 15% of the China's total respectively in Shanghai–Nanjing–Hangzhou. For other urban agglomerations, the average percentages of population and GDP during the same period always accounted from 2% to 9% (Fig. 2).

2.2. Data sources

The Version 4 DMSP-OLS Nighttime Lights Time-series (V4DNLTS) dataset for 1997–2012 was obtained from the National Oceanic and Atmospheric Administration's National Geophysical Data Center (NOAA/NGDC) website (<http://www.ngdc.noaa.gov/eog/dmsp.html>). This dataset consists of three data types: the nighttime stable light (NSL) data, cloud-free coverage and nighttime light data without further filtering. Among the three data types, the NSL data include lights from country-sides, towns, cities and other sites with persistent lighting and present the annual average brightness in units of 6 bits digital numbers (DN) ranging from 0 to 63. They cover an area of –180 to 180 degrees in longitude and –65 to 75 degrees in latitude, at a spatial resolution of 1 km. In this study, we projected the global NSL datasets into the Lambert Azimuthal Equal Area Projection, and clipped them to administrative boundaries of the study areas at different levels. Since the NSL data were collected by six different DMSP satellites (F10, F12, F14, F15, F16 and F18), they could not be directly used to map CO₂ emissions due to the lack of continuity and comparability [36–39]. An approach for calibrating time-series NSL data developed by Cao et al. [40] was employed to reduce the discrepancies.

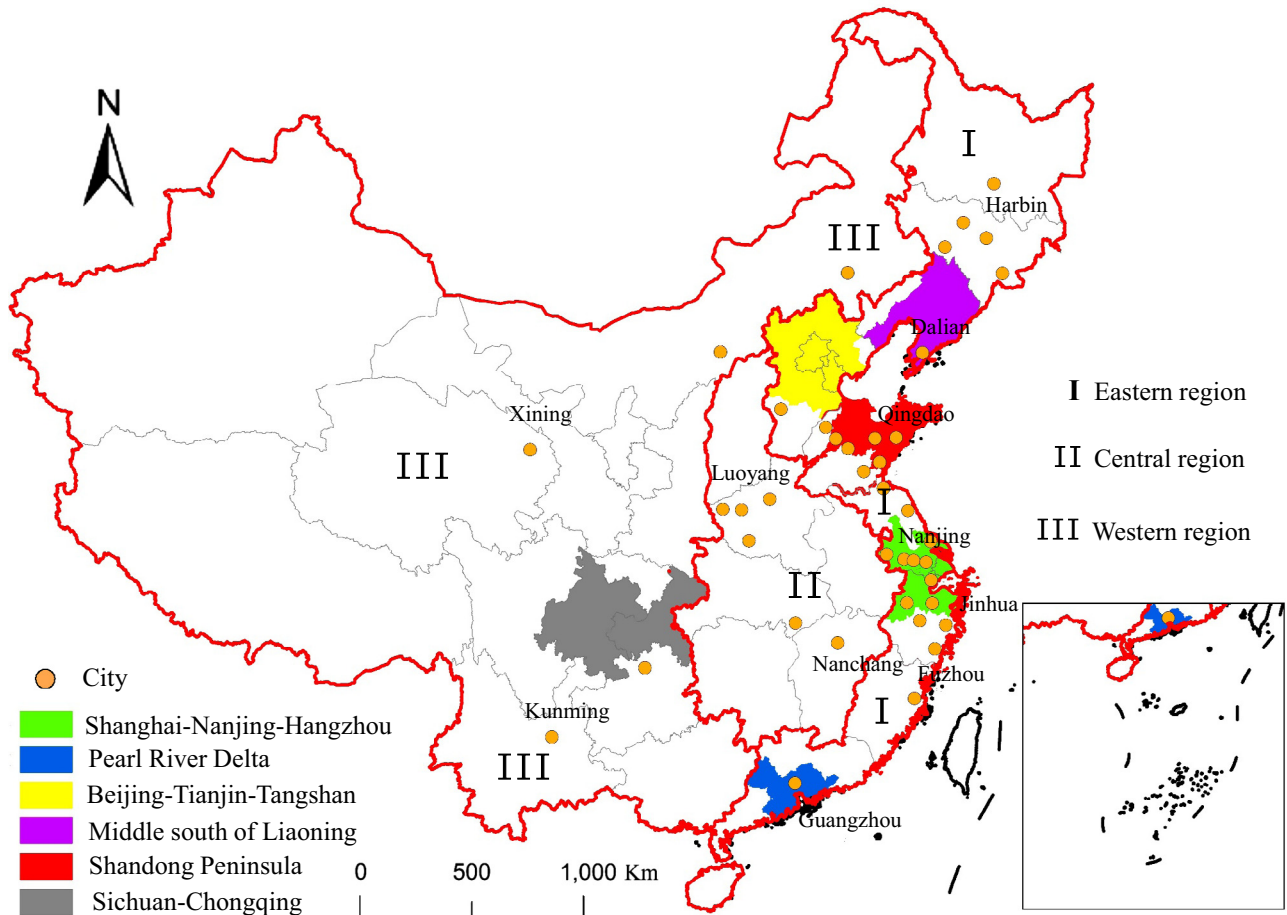


Fig. 1. The spatial distribution of study areas.

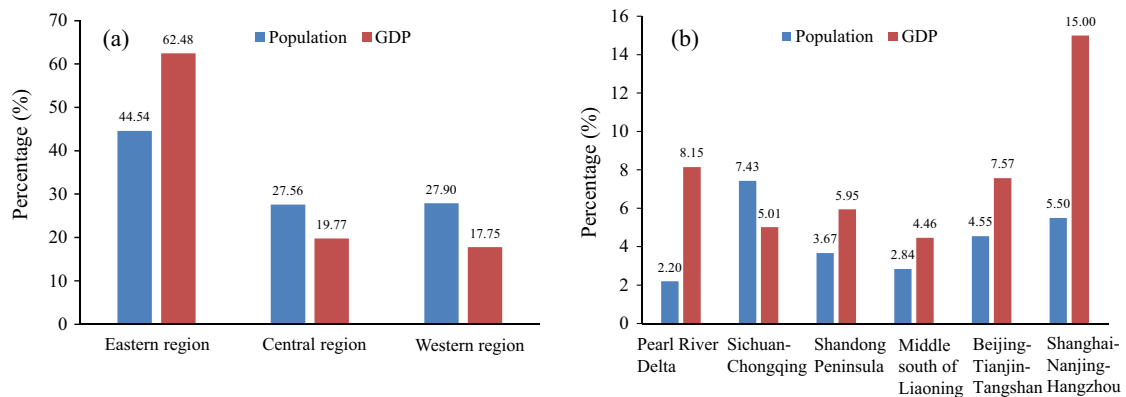


Fig. 2. The average percentages of population and GDP accounted the total in China for 1997–2012 at regional and urban agglomeration scales.

Statistical CO₂ emissions were estimated from energy consumption data using a unified standard method by the Intergovernmental Panel on Climate Change (IPCC) Guidelines [10,41–43]. This method involved four parameters, including the energy types, the amount of energy consumption, the average low-order calorific values (ALC), and the CO₂ emission coefficients (CEC). The energy consumption data were collected from the China Statistical Yearbook and corresponding City Statistical Yearbooks. The ALC were provided by the China Energy Statistical Yearbook. The CEC were derived from the National Greenhouse Gas Inventories of the 2006 IPCC (<http://www.ipcc.ch>). In addition, the administrative

boundary data for provinces, and cities in China were extracted from National Geomatics Center of China (<http://ngcc.sbsm.gov.cn>). A brief description of CO₂ emission-related data is listed in Table 1.

3. Methodology

Modeling CO₂ emissions at 1 km resolution using the NSL data is based on a hypothesis that a more developed area generally has brighter lights and larger CO₂ emissions. In other words, the

Table 1
Description of CO₂ emission related-data used in this study.

Data	Data description	Year	Source
Energy consumption data	Annual total data (10 ⁴ t) of eight energy types – coal, coke, crude oil, gasoline, coal oil, diesel oil, fuel oil and natural gas – for 30 provinces and 40 cities	1997–2012	China Energy Statistical Yearbook and corresponding City Statistical Yearbooks
ALC	Average low-order calorific values used as parameters to estimate CO ₂ emissions (kJ/kg)	2012	China Energy Statistical Yearbook
CEC	CO ₂ emission coefficients used as parameters to estimate CO ₂ emissions (kgCO ₂ /TJ)	2006	The National Greenhouse Gas Inventories of 2006 IPCC
Administrative boundaries	Shape files of provinces, cities in China	2008	National Geomatics Center of China

DN value of a pixel is positively correlated to CO₂ emissions from the pixel location on the ground [28]:

$$NC_c = aD_c + b \quad (1)$$

where NC is estimated CO₂ emissions, c is a specific pixel, D is the DN value of that pixel, a is a regression coefficient, and b is a intercept. Due to lack of the detailed CO₂ emissions at the pixel level, we assumed that the positive correlation between the DN values and statistical CO₂ emissions was constant within a specific province. Consequently, the statistical CO₂ emissions and total nighttime light (TNL) extracted at the provincial level were used to calculate the coefficient (a) and intercept (b) for each pixel within a province.

In this study, panel data analysis was adopted to establish a series of regression models for estimating CO₂ emissions at 1 km resolution. With the consideration of the regional difference in socioeconomic status, industrial structures and energy efficiencies, we conducted panel data analyses separately at regional scale (Eastern region, Central region and Western region). The procedures were as follows: firstly, panel unit root tests were conducted to validate the stationarity of the variables, including statistical CO₂ emissions and TNL at the provincial level; secondly, panel co-integration tests were used to determine if there were a long-run relationship between the variables; finally, statistical CO₂ emissions were further used to correct the panel regression models for improving estimation accuracy. These steps are described in detail in the following sections and presented at the flowchart in Fig. 3. Descriptions of Step I and II of the flowchart can be found in the earlier part of data sources section. A natural logarithm transformation was implemented for all data to avoid heteroskedasticity and non-stationarity phenomena before conducting panel data analysis.

3.1. Panel unit root tests

While some time series data might present a common change trend, the sequences in question might not have a direct correlation due to their non-stationary nature [29]. If we conducted a regression on these series data, the results could be meaningless despite having a high correlation coefficient value. To avoid this spurious regression, we examined the stationary nature of the variables before the panel data models were established [33]. In this study, two improved panel unit root tests, namely the Levin–Lin–Chu (LLC) test [44] and the ADF-Fisher test [45], were used to assess the stationarity of variables.

3.2. Panel co-integration tests

If the results of the panel unit root tests indicated that the variables were integrated of order one, then the next step was to employ panel co-integration tests to determine whether a long-run relationship existed between the variables. In this study, seven residual-based null of no cointegration panel test statistics that allowed for heterogeneous intercepts and trend coefficients

across-section were applied [46]. Of these seven statistics, the panel ν -statistic, panel r -statistic, panel PP-statistic and panel ADF-statistic pool the autoregressive coefficients across different numbers based on the within-dimension approach. The other three statistics, including Group rho-Statistic, Group PP-Statistic and Group ADF-Statistic, pool the residuals of the regression along the between dimension approach [3]. Detailed description of these tests and relevant critical values can be found in Pedroni's paper [46].

3.3. Panel data models

The regression models of panel data analysis can be categorized into three types: pooled regression model, variable intercepts and constant coefficients model, and variable intercepts and variable coefficients model. The formulas are:

$$y_{it} = \alpha + \beta x_{it} + \mu_{it} \quad (i = 1, 2, \dots, N; t = 1, 2, \dots, T) \quad (2)$$

$$y_{it} = \alpha_i + \beta x_{it} + \mu_{it} \quad (i = 1, 2, \dots, N; t = 1, 2, \dots, T) \quad (3)$$

$$y_{it} = \alpha_i + \beta_i x_{it} + \mu_{it} \quad (i = 1, 2, \dots, N; t = 1, 2, \dots, T) \quad (4)$$

where α_i is the intercept for specifying as fixed or random effects; Similarly, β_i can also be expressed as a fixed or random effect; and μ_{it} is the error term.

There are two main hypothesis to determine which specific model should be chosen:

$$H_1 : \beta_1 = \beta_2 = \dots = \beta_N \quad (5)$$

$$H_2 : \alpha_1 = \alpha_2 = \dots = \alpha_N, \quad \beta_1 = \beta_2 = \dots = \beta_N \quad (6)$$

Whether or not the hypothesis is accepted is based on F -test. If hypothesis H_2 is accepted, Eq. (2) is selected, otherwise it is necessary to test hypothesis H_1 . If hypothesis H_1 is then accepted, Eq. (3) is available; otherwise, Eq. (4) is chosen. Next, a critical step is to choose an effect model (either fixed model or random model), which has been debated among researchers. This study adopted fixed effect model that more likely produced reasonable outcomes under any circumstances [47].

3.4. Estimation and classification of CO₂ emissions

Once the linear correlation was confirmed by panel data analysis, it was valid to use the NSL data as a proxy to estimate CO₂ emissions at the pixel level. In addition, to limit the errors within a provincial unit, we further applied the statistical CO₂ emissions of each province to correct the estimated models:

$$CC_{ct} = SC_{it} \times (NC_{ct} \div NC_{it}) \quad (7)$$

where CC is the corrected CO₂ emissions of a specific pixel; SC is the statistical CO₂ emissions, and NC represents the estimated CO₂ emissions; c and i are a specific pixel and provincial unit, respectively.

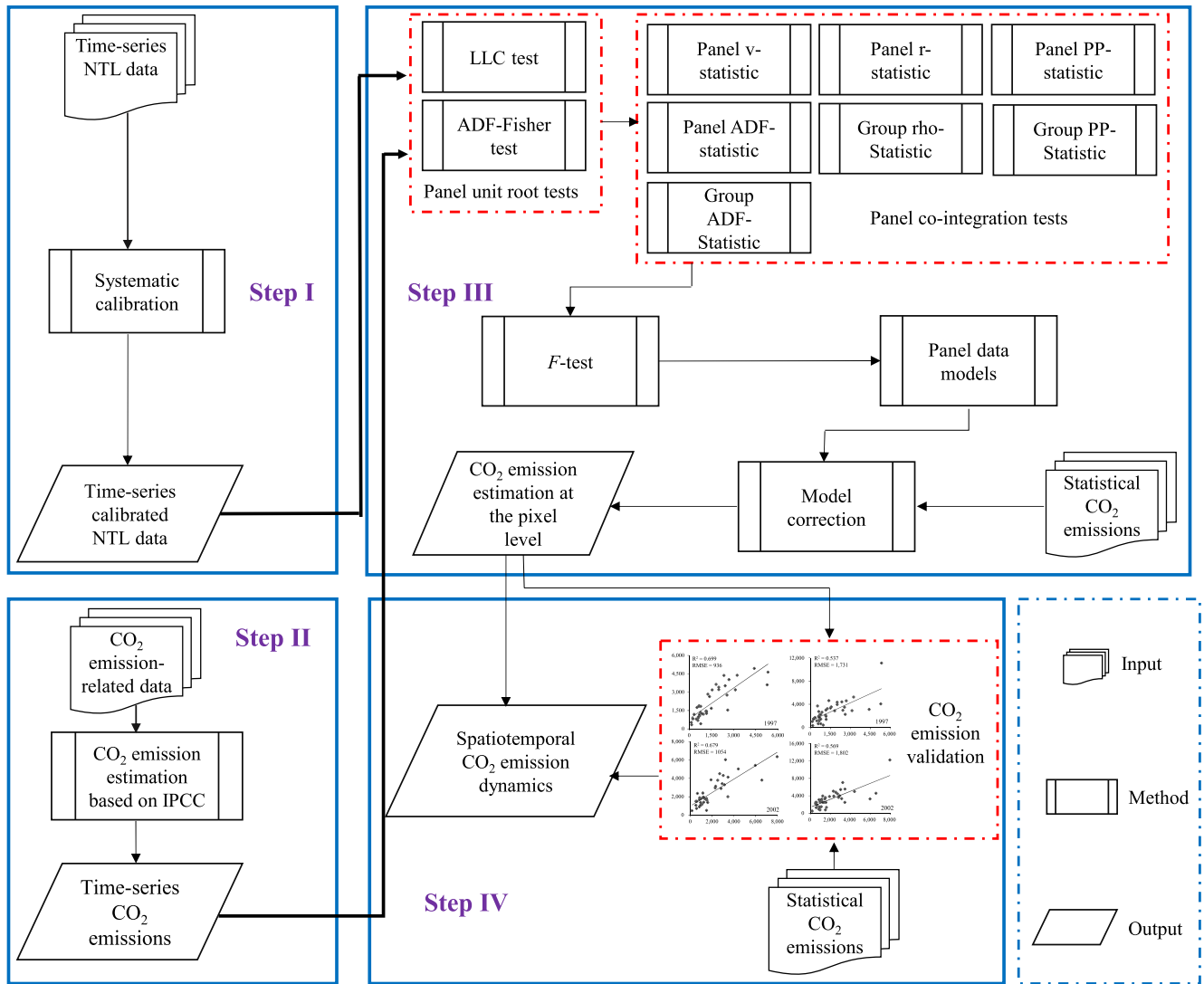


Fig. 3. Flowchart of methodology for modeling CO₂ emissions in China.

The Natural Break method [48,49] was applied to classify the spatiotemporal CO₂ emission maps. The temporal variation of CO₂ emissions for 1997–2012 was classified into four types: no-obvious-growth, low-growth, moderate-growth and high-growth. In addition, the average CO₂ emissions, which were used to quantify the spatial variations of CO₂ emissions for 1997–2012, were grouped into five grades: low, relatively-low, medium, relatively-high and high. Note that there are many ways to classify CO₂ emissions, The Natural Break method was chosen as the purpose

here was to investigate statistical variations in different areas of China, and it provides the smallest variances between categories, without influence of artificial factors [48,49].

4. Results

The results of this study are presented in two sections: firstly the results from panel data analysis at regional level; then the

Table 2
Results of panel unit root tests.

Region	Variable	Levin–Lin–Chu test		ADF-Fisher test	
		Level	First difference	Level	First difference
Eastern region	CO ₂ emissions	-0.5936	-6.5285***	6.9321	82.1996***
	TNL	-3.8232***	-9.0982***	19.1979	86.3568***
Central region	CO ₂ emissions	0.3178	-4.9525***	4.4392	31.0069***
	TNL	-1.6035*	-6.4083***	7.8952	39.0727***
Western region	CO ₂ emissions	4.3427	-5.7221***	8.0881	57.1190***
	TNL	-2.1909**	-7.5972***	15.1636	68.2183***

* Significant at 10% level.
 ** Significant at 5% level.
 *** Significant at 1% level.

spatiotemporal dynamics of CO₂ emissions from national scale down to regional and urban agglomeration scales.

4.1. Results of panel data analysis

4.1.1. Results of panel unit root tests

Table 2 lists the results of the LLC test and the ADF-Fisher test. For LLC test, TNL is stationary at the level in the Eastern region, Central and Western regions, rejecting the null hypothesis of non-stationary at less than 10% significance level. CO₂ emissions are not stationary at the level in these three regions. For the ADF-Fisher test, CO₂ emissions and TNL present panel non-stationary at the level. When the first difference is taken, all variables reject the null hypothesis of non-stationary at the 1% significance level. Therefore, CO₂ emissions and TNL are integrated at an order of one which means all the variables are stationary.

4.1.2. Results of panel co-integration tests

Table 3 shows that although the Panel ν -statistic, Panel rho-statistic, Panel PP-statistic, Group rho-statistic and Group PP-statistic of variables accept the null hypothesis of no co-integration in some regions, the other two statistics reject the hypothesis in all three regions. We followed Örsal's findings [50] that the Panel ADF-statistic performs better than the other six statistics, and so based our results of panel co-integration tests on the Panel ADF-statistic. This statistic rejects the null hypothesis of no co-integration at the 5% significance level and demonstrates that CO₂ emissions maintained a long-term equilibrium relationship with TNL in the three regions during the study period.

4.1.3. Parameter estimation of the panel models

According to the F -test, the variable intercepts and variable coefficients model was required in this study. The relationship between TNL and statistical CO₂ emissions was expressed by the individual fixed-varying coefficient model which performed better than other models. The models for three regions were as follows:

Eastern region:

$$NC_{it} = -29.9731 + \alpha_i + \beta_i TNL_{it} \quad (i = 1, 2, \dots, 13, t = 1, 2, \dots, 16) \quad (8)$$

Central region:

$$NC_{it} = -22.7140 + \alpha_i + \beta_i TNL_{it} \quad (i = 1, 2, \dots, 6, t = 1, 2, \dots, 16) \quad (9)$$

Western region:

$$NC_{it} = -14.9188 + \alpha_i + \beta_i TNL_{it} \quad (i = 1, 2, \dots, 11, t = 1, 2, \dots, 16) \quad (10)$$

in Eq. (8)–(10), the intercepts α_i and coefficients β_i alter with provinces, and are listed in Table 4 for calculating CO₂ emissions at the pixel level based on Eq. (7).

Table 4

Parameter estimation by panel data models. Note: due to the data availability, Qinghai and Tibet are treated as a uniform unit in this study.

Regions	Provinces	β_i	α_i
Eastern region	Beijing	1.3838	21.15581
	Tianjin	3.0274	0.379339
	Hebei	4.4574	-22.82547
	Liaoning	2.9793	-0.39951
	Jilin	2.0633	12.46855
	Heilongjiang	1.4780	19.67013
	Shanghai	1.9083	15.09531
	Jiangsu	2.1664	9.43719
	Zhejiang	1.6866	16.71677
	Fujian	3.6087	-8.714073
	Shandong	4.3104	-21.81738
	Guangdong	4.3514	-23.38404
	Hainan	4.6378	-17.78263
Central region	Shanxi	4.0607	-23.3772
	Anhui	1.7250	9.5782
	Jiangxi	1.1905	16.9392
	Henan	3.5061	-16.2779
	Hubei	2.3050	2.2554
	Hunan	1.6754	10.8823
Western region	Inner Mongolia	2.2112	-4.3184
	Guangxi	2.3622	-6.7822
	Chongqing	1.0703	11.0754
	Sichuan	1.2408	8.5371
	Guizhou	1.2686	9.0101
	Yunnan	2.0361	-2.5321
	Shaanxi	2.3973	-7.4711
	Gansu	1.4710	5.7147
	Ningxia	2.4004	-4.8950
	Xinjiang	2.8174	-13.5879
	Qinghai	1.5418	5.2496
	Tibet	1.5418	5.2496

4.2. Spatiotemporal dynamics of CO₂ emissions

The spatiotemporal dynamics of CO₂ emissions in China for 1997–2012 were mapped in Fig. 4. The high CO₂ emissions were clearly identified in coastal region such as the Beijing–Tianjin–Ta ngshan and Yangtze River Delta, with the low CO₂ emissions mainly located in the rural areas of the Western and Central regions. Significant spatiotemporal variations in China's CO₂ emissions could be seen clearly increasing and expanding during the past decades.

4.2.1. Spatiotemporal dynamics of CO₂ emissions at national scale

Fig. 5 maps the four types and five grades of CO₂ emissions in China for 1997–2012. The high-growth type was concentrated in coastal regions, some inland metropolitan areas and developed cities, including Shanghai, Tianjin, Beijing and provincial capitals (Fig. 5a). In other words, the growth of CO₂ emissions (about 8.6 billion tons) was concentrated in 7.28% of the total area of China. 92.72% of the total area of China showed no-obvious-growth types (Figs. 5a and 6a). Moreover, the spatial distribution of CO₂ emissions was very similar to the CO₂ emission growth in China (Figs. 5b and 6b). Most regions in China had relatively-low

Table 3

Results of panel co-integration tests.

Region	Panel ν -statistic	Panel rho-statistic	Panel PP-statistic	Panel ADF-statistic	Group rho-statistic	Group PP-statistic	Group ADF-statistic
Eastern region	1.6576**	-2.1694**	-2.6751***	-3.4055***	0.3215	-1.7211**	-4.6438***
Central region	1.6037*	0.9776	-0.3356	-2.2639**	2.0205	0.2345	-1.3715*
Western region	0.8391	-0.5416	-1.4481*	-2.6377***	0.6550	-1.2426	-3.5111***

* Significant at 10% level.

** Significant at 5% level.

*** Significant at 1% level.

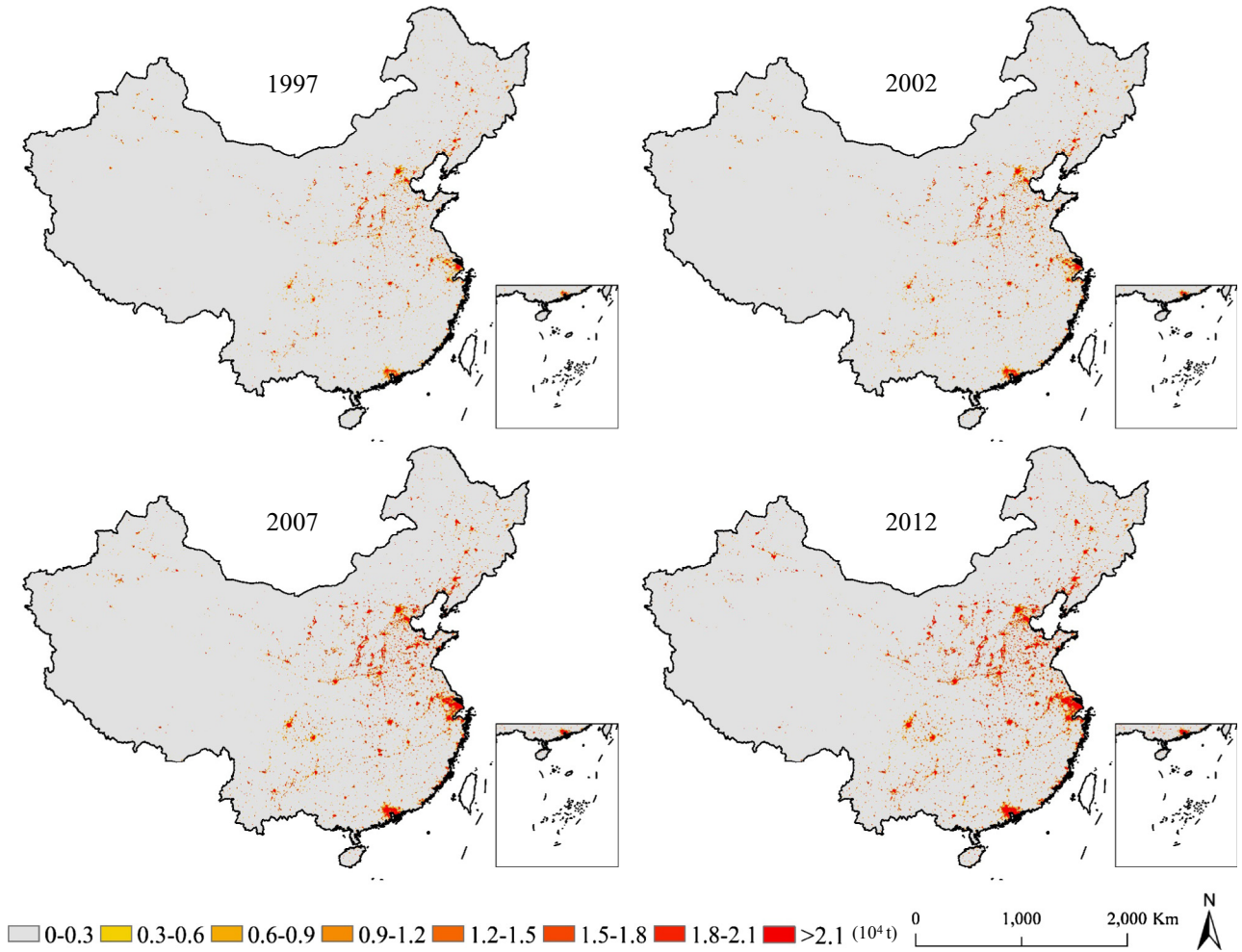


Fig. 4. Maps of CO₂ emissions in China for 1997–2012. Note: the negative values of preliminary CO₂ emission estimation are presented as zero.

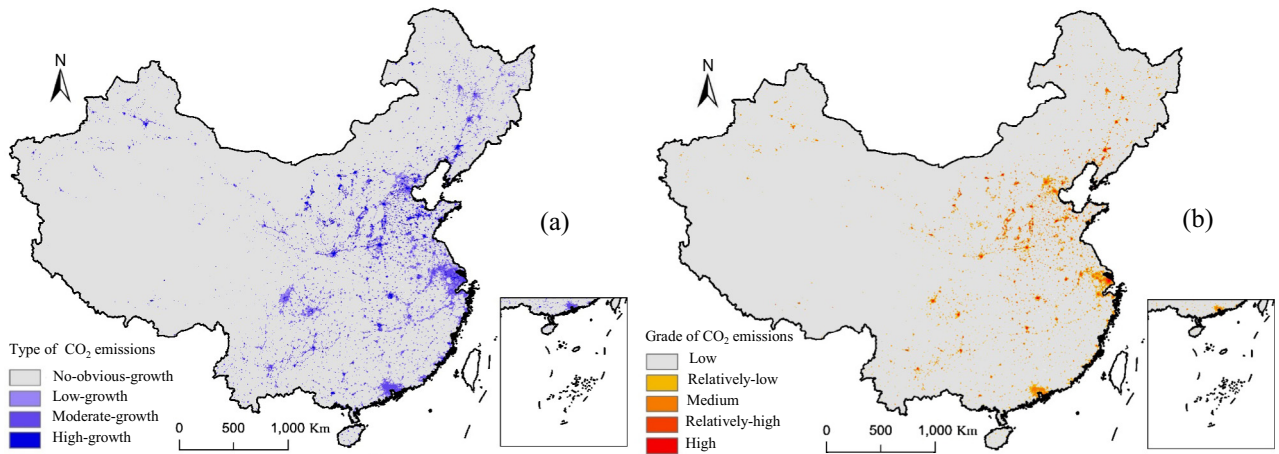


Fig. 5. (a) Temporal variations of CO₂ emissions in China for 1997–2012 and (b) spatial variations of CO₂ emissions in China for 1997–2012. Note: the negative growth is viewed as a type of no-obvious-growth.

to low grades of CO₂ emissions, covering 173,616 km² (1.84%) and 9,165,063 km² (96.86%) of the total area of China, respectively. On the other hand, the high, relatively-high and medium grades were mainly distributed in coastal regions, covering 0.12%, 0.34% and 0.84% of the total area of China, respectively (Fig. 6b).

4.2.2. Spatiotemporal dynamics of CO₂ emissions at regional scale

Fig. 7 contained the areal percentage of each type and grade in the three regions. The high-growth type was mainly concentrated in the Eastern region and accounted for 46.56% of the total area of that type (Fig. 7a). Conversely, no-obvious-growth type was

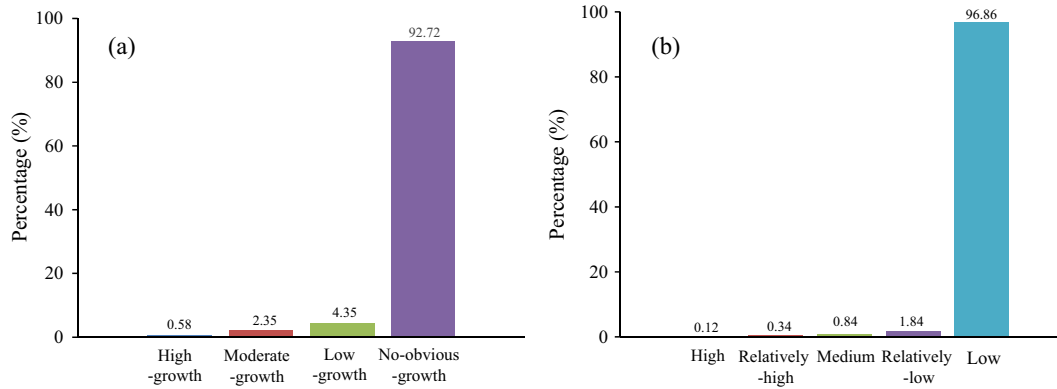


Fig. 6. (a) Areal percentage of each type in China and (b) areal percentage of each grade in China.

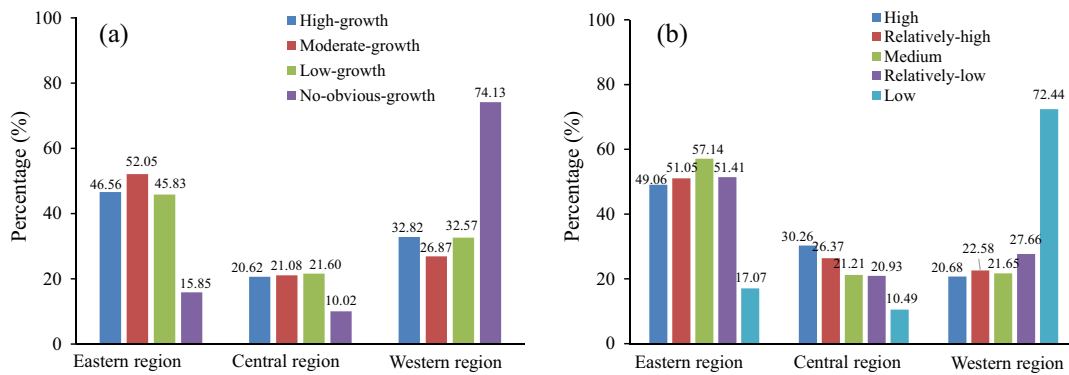


Fig. 7. (a) Areal percentage of each type in the three regions and (b) areal percentage of each grade in the three regions.

mainly located in the Western region and accounted for 74.13% of the total area of that type. In addition, 49.06% of high grade and 51.05% of relatively-high grade were concentrated in the Eastern region, with clearly lower concentrations in the Western and Central regions. Again, the distribution of five grades of CO₂ emissions was relatively uniform in the Central region. In contrast, the Western region was dominated by low grade emissions (>72%).

4.2.3. Spatiotemporal dynamics of CO₂ emissions at urban agglomeration scale

During past 16 years, the six urban agglomerations accounted for 7.75% of the total area in China, yet contributed 37.12% of

CO₂ emissions. Although their CO₂ emissions increased continuously for 1997–2012, the differences in growth rates and amounts were huge. In terms of percentage of total areas, no-obvious-growth type was 81.97% in Middle south of Liaoning. The growth of CO₂ emissions was 31.41% in Shanghai–Nanjing–Hangzhou and 17.97% in Pearl River Delta showed a low growth type, whereas 8.70% of Shandong Peninsula presented high growth type (Fig. 8a). Moreover, the low grade of CO₂ emissions was 94.58% in Sichuan–Chongqing. Besides, the relatively-low grade of CO₂ emissions was 20.14% in Shanghai–Nanjing–Hangzhou and 13.97% in Pearl River Delta. The Middle south of Liaoning was the urban agglomeration which had the high CO₂ emissions, with the high grade covering 1.63% (Fig. 8b).

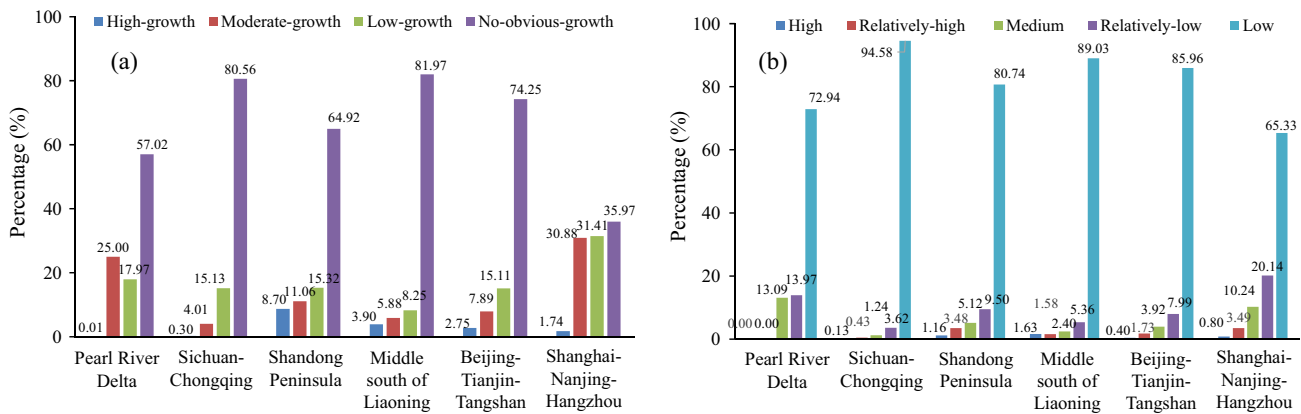


Fig. 8. (a) Areal percentage of each type within the six urban agglomerations and (b) areal percentage of each grade within the six urban agglomerations.

5. Discussion

5.1. Validation of spatiotemporal CO₂ emission dynamics

Panel data analysis proposed in this study utilized NSL data and statistical CO₂ emissions and was found to be an effective way for timely modeling spatiotemporal CO₂ emissions at 1 km resolution in China. To assess the accuracy of our results, comparisons among panel data analysis, linear regression model, power regression model and lg–lg regression model for CO₂ emission estimation were evaluated in this study. Based on data availability, we collected statistical CO₂ emission data for 1997, 2002, 2007 and 2012 of 40 cities (Fig. 1) which are distributed relatively evenly on the mainland China, and calculated the total CO₂ emissions for each city from the spatiotemporal CO₂ emission maps using different model. Two indicators were used to evaluate the accuracies of the spatial distributions of CO₂ emissions – the coefficient of determination R^2 and root-mean-square error (RMSE). Fig. 9 shows that: the R^2 values between the estimated CO₂ emissions from panel data analysis and statistical CO₂ emissions are higher than those from other models. Figure also tells that panel data analysis produces significantly lower RMSEs than those models. These results suggest panel data analysis performed better than other three models to estimate CO₂ emissions at 1 km resolution in China.

Although the simple regression methods have been widely applied to estimate CO₂ emissions, they should integrate multiple sources to accurate map CO₂ emissions. In addition, these models could not demonstrate that the positive relationship between NSL data and statistical CO₂ emissions was spurious or true. In this study, panel data analysis showed that NSL data and CO₂ emissions were integrated at an order of one and exhibited a long-run relationship, which demonstrated a true correlation between NSL data and statistical CO₂ emissions in China at the provincial level during the study period. Meanwhile, panel data analysis endowed a series of regression models to model CO₂ emissions efficiently across spatial and temporal dimensions without any ancillary data.

The validity test and comparison analyses have well proved the ability of the panel data analysis to model CO₂ emissions, but some problems still exist in this study. Firstly, the reliability of the statistical energy data is a key factor influencing CO₂ emission estimation. It was reported that estimation of CO₂ emissions in China might be off by as much as 20% [51], with coal consumption accounting for 71% of the emissions discrepancy [52]. Improving the reliability of statistical energy data in China would surely increase the accuracy of the method proposed in this study. In addition, since the NSL data have a set of shortcomings, such as saturation on bright lights, six bit quantization, there is considerable rooms for improving data quality, and applying more methods to

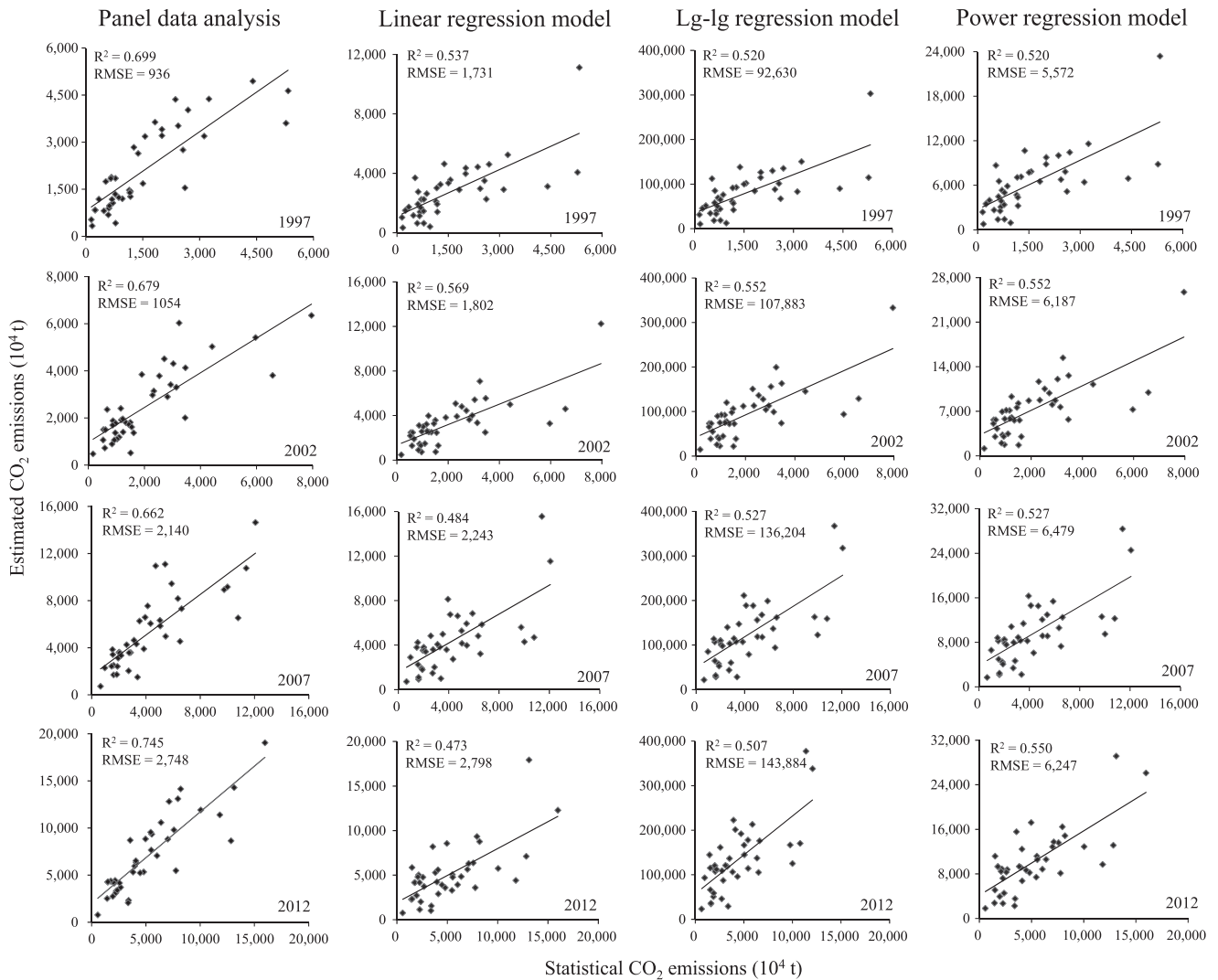


Fig. 9. Accuracy assessment between the estimated CO₂ emissions and statistical CO₂ emissions.

the data correction process [16]. In summary, the NSL data, using the panel data analysis, provides a new way of understanding spatiotemporal CO₂ emission dynamics in China at 1 km resolution where CO₂ emissions have been difficult to estimate due to lack of the statistical energy data.

5.2. Outlook and suggestions for China's CO₂ emission mitigation

The rapid increase of China's CO₂ emissions not only has a negative impact on its sustainable development, but also influences the long term stability of global climate. In this context, Chinese government pledged to reduce CO₂ emission intensity by 40–45% below the 2005 level by 2020 to reach the international climate agreement of Copenhagen in 2009. Furthermore, in 2015, more ambitious target was set by reducing 60–65% of CO₂ emission intensity by 2030 comparing to the 2005 level. The new target would put a greater pressure on China to substantially reduce its CO₂ emissions, especially in Eastern region. The CO₂ emission mitigation might compromise the ongoing economic developments in Central and Western region.

It is definitely a great challenge to Chinese central and local governments to achieve above targets without diverting the economic development. Considering the huge economic gaps among regions, different mitigation strategies are needed for different regions to cope with their statuses of economic development. As Eastern region has already been at a relatively high stage of economic development, the mitigation strategies of CO₂ emissions can focus on optimizing the industrial structures. High-tech manufacturing, financial industries with low energy demanding and low CO₂ emissions should be encouraged and supported. High CO₂ emission industries, such as metal, chemical, mining, and coal powers, should be replaced or upgraded. The Central and Western regions are at an early stage of economic development. It is not feasible and realistic to completely alter their industrial structures in a short term. It is probably more effective to reduce CO₂ emissions by improving energy efficiencies of utilization, transformation and recycling processes. Besides, corresponding policies and laws should be made to facilitate CO₂ emission mitigation in all regions. For instance, higher taxations should be applied to high CO₂ emission industries in Eastern region, while taxation deduction, loan preferences and financial subsidies should be awarded to industries which developed energy-saving and low CO₂ emission technologies.

6. Conclusions

This study proposed panel data analysis to model spatiotemporal CO₂ emission dynamics at a higher resolution in China by integrating remotely sensed imagery with statistic data of CO₂ emissions. This approach has demonstrated that there was a true positive correlation between NSL data and statistical CO₂ emissions at the provincial level from 1997 to 2012. The spatial model effectively estimated CO₂ emissions at the 1 km pixel level. Spatiotemporal CO₂ emission dynamics were evaluated from national scale down to regional and urban agglomeration scales. The model outputs clearly presented the great variations of CO₂ emissions among different regions. The high growth type and high grade of CO₂ emissions were mainly distributed in the Eastern region, Shandong Peninsula and Middle south of Liaoning, with significant lower concentrations in the Western region, Central region and Sichuan–Chongqing.

The results of this study will improve the understanding of regional discrepancies of spatiotemporal CO₂ emission dynamics at the multiple scales, and provide a scientific basis for policy-making on viable CO₂ emission mitigation policies. With the release of first global Suomi National Polar-orbiting Partnership (NPP) Visible Infrared Imaging Radiometer Suite (VIIRS) nighttime

light composite data at a 0.5 km resolution, further improvement on spatiotemporal CO₂ emission dynamics using panel data analysis becomes possible.

Acknowledgements

This work is supported by the National Natural Science Foundation of China (No. 41471449), the Natural Science Foundation of Shanghai (No. 14ZR1412200), the Innovation Program of Shanghai Municipal Education Commission (No. 15ZZ026), the Fundamental Research Funds for the Central Universities of China, and the China Scholarship Council (No. 201406140007). The authors also wish to thank their colleagues Susan Cuddy for her helpful suggestions.

References

- [1] Wei Y, Wang L, Liao H, Wang K, Murty T, Yan J. Responsibility accounting in carbon allocation: a global perspective. *Appl Energy* 2014;130:122–33.
- [2] Lu H, Liu G. Spatial effects of carbon dioxide emissions from residential energy consumption: a county-level study using enhanced nocturnal lighting. *Appl Energy* 2014;131:297–306.
- [3] Ou J, Liu X, Li X, Chen Y. Quantifying the relationship between urban forms and carbon emissions using panel data analysis. *Landsc Ecol* 2013;28:1889–907.
- [4] Bakhtyar B, Ibrahim Y, Alghoul MA, Aziz N, Fudholi A, Sopian K. Estimating the CO₂ abatement cost: substitute price of avoiding CO₂ emission (SPA) by renewable energy's feed in tariff in selected countries. *Renew Sustain Energy Rev* 2014;35:205–10.
- [5] Ozturk I, Acaravci A. CO₂ emissions, energy consumption and economic growth in Turkey. *Renew Sustain Energy Rev* 2010;14:3220–5.
- [6] He C, Ma Q, Li T, Yang Y, Liu Z. Spatiotemporal dynamics of electric power consumption in Chinese Mainland from 1995 to 2008 modeled using DMSP/OLS stable nighttime lights data. *J Geogr Sci* 2012;22:125–36.
- [7] Wang N, Chang Y. The development of policy instruments in supporting low-carbon governance in China. *Renew Sustain Energy Rev* 2014;35:126–35.
- [8] Wang K, Wei Y. China's regional industrial energy efficiency and carbon emissions abatement costs. *Appl Energy* 2014;130:617–31.
- [9] Su Y, Chen X, Li Y, Liao J, Ye Y, Zhang H, et al. China's 19-year city-level carbon emissions of energy consumptions, driving forces and regionalized mitigation guidelines. *Renew Sustain Energy Rev* 2014;35:231–43.
- [10] Cheng Y, Wang Z, Ye X, Wei Y. Spatiotemporal dynamics of carbon intensity from energy consumption in China. *J Geogr Sci* 2014;24:631–50.
- [11] Geng Y, Tian M, Zhu Q, Zhang J, Peng C. Quantification of provincial-level carbon emissions from energy consumption in China. *Renew Sustain Energy Rev* 2011;15:3658–68.
- [12] Kamalinia S, Shahidehpour M, Wu L. Sustainable resource planning in energy markets. *Appl Energy* 2014;133:112–20.
- [13] Clarke-Sather A, Qu J, Wang Q, Zeng J, Li Y. Carbon inequality at the sub-national scale: a case study of provincial-level inequality in CO₂ emissions in China 1997–2007. *Energy Policy* 2011;39:5420–8.
- [14] Gingrich S, Kuskova P, Steinberger JK. Long-term changes in CO₂ emissions in Austria and Czechoslovakia—Identifying the drivers of environmental pressures. *Energy Policy* 2011;39:535–43.
- [15] Cao X, Wang J, Chen J, Shi F. Spatialization of electricity consumption of China using saturation-corrected DMSP-OLS data. *Int J Appl Earth Observ Geoinf* 2014;28:193–200.
- [16] Shi K, Yu B, Huang Y, Hu Y, Yin B, Chen Z, et al. Evaluating the ability of NPP-VIIRS nighttime light data to estimate the gross domestic product and the electric power consumption of China at multiple scales: a comparison with DMSP-OLS data. *Rem Sens* 2014;6:1705–24.
- [17] Zhao N, Ghosh T, Samson EL. Mapping spatio-temporal changes of Chinese electric power consumption using night-time imagery. *Int J Remote Sens* 2012;33:6304–20.
- [18] Yu B, Shi K, Hu Y, Huang C, Chen Z, Wu J. Poverty evaluation using NPP-VIIRS nighttime light composite data at the county level in China. *IEEE J Select Top Appl Earth Observ Rem Sens* 2015;8:1217–29.
- [19] Shi K, Yu B, Hu Y, Huang C, Chen Y, Huang Y, et al. Modeling and mapping total freight traffic in China using NPP-VIIRS nighttime light composite data. *GISci Rem Sens* 2015;52:274–89.
- [20] Shi K, Huang C, Yu B, Yin B, Huang Y, Wu J. Evaluation of NPP-VIIRS night-time light composite data for extracting built-up urban areas. *Rem Sens Lett* 2014;5:358–66.
- [21] Li X, Chen F, Chen X. Satellite-observed nighttime light variation as evidence for global armed conflicts. *IEEE J Select Top Appl Earth Observ Rem Sens* 2013;6:2302–15.
- [22] Yu B, Shu S, Liu H, Song W, Wu J, Wang L, et al. Object-based spatial cluster analysis of urban landscape pattern using nighttime light satellite images: a case study of China. *Int J Geogr Inf Sci* 2014;28:2328–55.
- [23] Li X, Chen X, Zhao Y, Xu J, Chen F, Li H. Automatic intercalibration of night-time light imagery using robust regression. *Rem Sens Lett* 2013;4:45–54.
- [24] Chen Z, Yu B, Hu Y, Huang C, Shi K, Wu J. Estimating house vacancy rate in Metropolitan areas using NPP-VIIRS nighttime light composite data. *IEEE J Select Top Appl Earth Observ Rem Sens* 2015;8:2188–97.

- [25] Li X, Xu H, Chen X, Li C. Potential of NPP-VIIRS nighttime light imagery for modeling the regional economy of China. *Rem Sens* 2013;5:3057–81.
- [26] Prasad VK, Kant Y, Gupta PK, Elvidge C, Badarinath KVS. Biomass burning and related trace gas emissions from tropical dry deciduous forests of India: a study using DMSP-OLS data and ground-based measurements. *Int J Rem Sens* 2002;23:2837–51.
- [27] Propastin P, Kappas M. Assessing satellite-observed nighttime lights for monitoring socioeconomic parameters in the Republic of Kazakhstan. *GISci Rem Sens* 2012;49:538–57.
- [28] Meng L, Graus W, Worrell E, Huang B. Estimating CO₂ (carbon dioxide) emissions at urban scales by DMSP/OLS (Defense Meteorological Satellite Program's Operational Linescan System) nighttime light imagery: methodological challenges and a case study for China. *Energy* 2014;71:468–78.
- [29] Wang S, Fang C, Wang Y, Huang Y, Ma H. Quantifying the relationship between urban development intensity and carbon dioxide emissions using a panel data analysis. *Ecol Indic* 2015;49:121–31.
- [30] Wu J, Wang Z, Li WF, Peng J. Exploring factors affecting the relationship between light consumption and GDP based on DMSP/OLS nighttime satellite imagery. *Rem Sens Environ* 2013;134:111–9.
- [31] Chen Y, Li X, Zheng Y, Guan Y, Liu X. Estimating the relationship between urban forms and energy consumption: a case study in the Pearl River Delta, 2005–2008. *Landsc Urban Plan* 2011;102:33–42.
- [32] Baltagi B. *Econometric analysis of panel data*. John Wiley & Sons; 2008.
- [33] Wang S, Fang C, Guan X, Pang B, Ma H. Urbanisation, energy consumption, and carbon dioxide emissions in China: a panel data analysis of China's provinces. *Appl Energy* 2014;136:738–49.
- [34] Feyzioglu T, Swaroop V, Zhu M. A panel data analysis of the fungibility of foreign aid. *The World Bank Econ Rev* 1998;12:29–58.
- [35] Yaffee R. *A primer for panel data analysis*. Connect: Inf Technol NYU 2003.
- [36] He C, Shi P, Li J, Chen J, Pan Y, Li J, et al. Restoring urbanization process in China in the 1990s by using non-radiance-calibrated DMSP/OLS nighttime light imagery and statistical data. *Chin Sci Bull* 2006;51:1614–20.
- [37] Zhang Q, Seto KC. Mapping urbanization dynamics at regional and global scales using multi-temporal DMSP/OLS nighttime light data. *Rem Sens Environ* 2011;115:2320–9.
- [38] Small C, Pozzi F, Elvidge CD. Spatial analysis of global urban extent from DMSP-OLS night lights. *Rem Sens Environ* 2005;96:277–91.
- [39] Zhao N, Zhou Y, Samson EL. Correcting incompatible DN values and geometric errors in nighttime lights time-series images. *IEEE Trans Geosci Rem Sens* 2015;53:2039–49.
- [40] Cao Z, Wu Z, Kuang Y, Huang N. Correction of DMSP/OLS nighttime light images and its application in China. *J Geo-Inf Sci* 2015;17:1092–102 [in Chinese].
- [41] *Climate change 2007 the fourth assessment report of IPCC*. Cambridge: Cambridge University Press; 2007.
- [42] Aydin G. Modeling of energy consumption based on economic and demographic factors: the case of Turkey with projections. *Renew Sustain Energy Rev* 2014;35:382–9.
- [43] Bi J, Zhang R, Wang H, Liu M, Wu Y. The benchmarks of carbon emissions and policy implications for China's cities: case of Nanjing. *Energy Policy* 2011;39:4785–94.
- [44] Levin A, Lin C, James Chu C. Unit root tests in panel data: asymptotic and finite-sample properties. *J Economet* 2002;108:1–24.
- [45] Dickey DA, Fuller WA. Distribution of the estimators for autoregressive time series with a unit root. *J Am Statist Assoc* 1979;74:427–31.
- [46] Pedroni P. Critical values for cointegration tests in heterogeneous panels with multiple regressors. *Oxford Bull Econ Statist* 1999;61:653–70.
- [47] Zhang H, Jia Y. The new idea of panel data model. *J Quant Tech Econ* 2006:148–54 [in Chinese].
- [48] Xie H, Zou J, Peng X. Spatial–temporal difference analysis of cultivated land use intensity based on emergy in Poyang Lake Eco-economic Zone. *Acta Geogr Sin* 2012;67:889–902 [in Chinese].
- [49] Brewer CA, Pickle L. Evaluation of methods for classifying epidemiological data on choropleth maps in series. *Ann Assoc Am Geogr* 2002;92:662–81.
- [50] Örsal DDK. *Comparison of panel cointegration tests*. SFB 649 discussion paper; 2007.
- [51] Jiao L, Stone R. China looks to balance its carbon books. *Science* 2011;334:886–7.
- [52] Guan D, Liu Z, Geng Y, Lindner S, Hubacek K. The gigatonne gap in China's carbon dioxide inventories. *Nat Climate Change* 2012;2:672–5.